2018 7th IEEE International Conference on Biomedical
Robotics and Biomechatronics (Biorob)
Enschede, The Netherlands, August 26-29, 2018

# Intuitive Impedance Modulation in Haptic Control using Electromyography*

Kees van Teeffelen[1,2,3], Douwe Dresscher[1,2], Wietse van Dijk[1,3] and Stefano Stramigioli[2,4]

*Abstract*— **Humans have multiple ways to adapt their arm dynamics to the task they have to perform. One way of doing this is through co-contraction of antagonist muscles. In telemanipulation this ability is easily lost due to time delays, quantization effects, bandwidth or hardware limitations. In this work a new concept for telemanipulation is presented. The end-point stiffness of a (simulated) telerobot is controlled via a variable impedance controller. The end effector stiffness scales with an estimate of the co-contraction around the elbow of the teleoperator. The telemanipulation concept was evaluated with ten subjects that performed two telemanipulation tasks in six different conditions. Three impedance levels: low, high, and variable, and two delay settings. The first task was on positioning accuracy, the second task on impact minimization. We have shown that low and variable impedance performed significantly better on the force task than high impedance. We have also shown that high and variable impedance performed significantly better on the position task than low impedance. This shows that the human ability to control arm stiffness can effectively be transferred to a telemanipulated robot.**

## I. INTRODUCTION

The well-developed sensory and motor skills that humans possess allow them to modulate their force application and the compliance of their limbs to dexterously interact with the environment. This modulation involves the ability to change the arm dynamics by non-linear muscle properties, co-contraction and body posture. By modulating these dynamic properties, humans can adapt their manipulation tactic to the task at hand. Examples are increasing limb compliance in order to carefully handle delicate objects or decreasing limb compliance to reject disturbing forces ([1], [3], [8], [13], [14]).

In the field of telerobotics, an aim is to use a robot as a natural extension of a human operator. In manipulation, an approach to achieve this goal is haptic control of a robotic manipulator during which force feedback is provided to the operator. This forms a human-machine interaction which is aimed at projecting human manipulation skills to a remote environment ([4], [14]).

In a perfect implementation - one with optimal transparency - the dynamic properties of the human arm would indeed be projected on the robotic manipulator. However, in the presence of time delays the human reaction to changing dynamics will be delayed by the round-trip time of the communication channel ([7], [9], [11]). The delayed reaction negatively influences the projection of the dynamic properties of the human arm on the robotic manipulator. Human dexterity is (partly) lost in a telerobotics system with communication delays and this can lead to reduced task performance and increased interaction forces between the robot and the remote environment ([1], [3], [14]).

The aim of this work is to partially re-capture the projection of the dynamic properties of the human arm on the robotic manipulator. Muscle activation levels of the human operator are measured trough electromyography (EMG) and used to modulate the compliance of the controller at the slave side of a telerobotics system, as also done in [1], [4].

In this paper we test the following hypotheses:

1) Telemanipulation tasks that require high position accuracy are performed better with high impedance, and telemanipulation tasks that require impact minimization are performed better with low impedance. Although this is a well established understanding in the field, it also form a basis for the following hypotheses and is therefore explicitly evaluated.
2) The co-contraction levels are higher in a telemanipulation task that requires high positioning accuracy than for a task that requires impact minimization
3) Scaling the controller impedance with the co-contraction level of the user allows users to effectively change between high and low impedance control.

In order to test these hypotheses a telemanipulation setup was developed in which the impedance of the controller of the end effector in the telemanipulated environment was variable. With this setup, ten subjects performed two tasks with different impedance needs, under several controller impedance and delay conditions. The task performance was evaluated in order to validate our hypotheses.

This paper is structured as follows; In section II, related efforts to transfer human limb characteristics to a teleoperated environment are discussed. In section III, the controller design is discussed and in section IV, the experimental setup and the design of the experiments. The focus of this work is on the results and interpretation of user studies which are in sections V and VI, respectively.

## II. RELATED WORK

Several attempts that aimed at transferring human limb dynamics to a teleoperated environment were found in literature. Focus is placed on teleoperated robots (slave devices)

*This work was done in collaboration by the University of Twente and TNO in the i-Botics joint innovation center (www.i-botics.com)

[1]These authors contributed equally to the work
[2]Faculty of Electrical Engineering, Mathematics and Computer Science, University of Twente, Postbus 217, 7500 AE Enschede, The Netherlands
[3]TNO (Netherlands Organisation for Applied Scientific Research), Postbus 3005, 2316 ZL Leiden, The Netherlands
[4]ITMO University, Russia

978-1-5386-8183-1/18/$31.00 ©2018 IEEE

that are controlled by human operators through a haptic device (master device) which presents information on the interaction forces at the remote site through force feedback. [4] conclude on positive results for the use of EMG, claiming that they were able to control a teleoperated robot more intuitively while at the same time increasing the tracking performance. The effectiveness of the approach was not reported in the research. Further indications that EMG can be used to identify human limb dynamics are presented by [1]. Although this research presents the use of EMG as an alternative to force feedback in telemanipulation systems, it does show the extent to which EMG can be used in estimating the human limb characteristics. The research shows an identification method for mass, stiffness and damping properties of the human arm in 3D, using EMG data from six relevant muscles.

Besides the use of EMG, other methods for estimating human dynamic characteristics have been applied in combination with force feedback in teleoperated robots. Research presented by [14] shows the use of a gripper on the master device that is able to measure the grip pressure of the user and relates this data to the desired behavior of the teleoperated robot. A tighter grip should then result in less compliant behavior of the robot. This research shows clear benefits of using the variable compliant control on the robotic telemanipulation system, mainly in reducing interaction forces in several situations.

Further research on estimating the desired robotic behavior based on the human characteristics was found in [8]. The author used active vibrations of the master device to measure the response of the human arm. Based on this response the dynamic properties of the arm can be estimated continuously and they suggest that this estimation can be used in a telemanipulation system with variable compliance. [3] related the robotic behavior to the load conditions as would be done by humans as well and finally, [13] related the desired robotic behavior to the recorded posture of the operator. Although these last publications show similarities in the addressed problem, none of them show clear experimental results on the effects of their control approaches.

## III. Controller Design

### A. Controller

A controller was designed that links a slave device to a master device. Fig. 1 shows a schematic representation of this controller design. In this figure, the human arm with impedance properties $K_h$ and $D_h$ with master device and the slave device can be distinguished.

The master slave device are connected through a (simulated) communication line and an impedance controller represented by a Cartesian spring with modulated stiffness $K(\eta)$ and joint damping with modulated damping ratio $D(\eta)$. The force generated by the Cartesian spring, $F_{K,s}$, is calculated based on the slave position, $X_s$, and the position of the master device, $X_m$:

$$F_{K,s} = K(\eta)(\widetilde{X}_m - X_s) \tag{1}$$

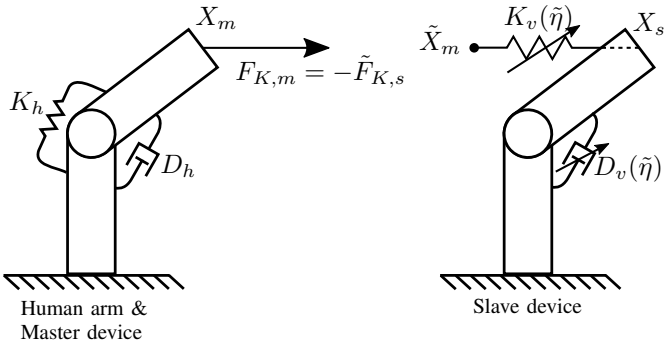


Fig. 1: Schematic representation of the designed haptic telemanipulation system. It is capable of modulating the dynamic characteristics of its control by the estimated co-contraction level $\eta$ computed with the relevant EMG data.

Where the tilde denotes that it is not an exact representation of the master position due to time delays. The force that is applied by the Cartesian spring to the slave device is used to generate force feedback, $F_{K,m}$, equal to:

$$F_{K,m} = -\widetilde{F}_{K,s} \tag{2}$$

Where the tilde denotes that it is not an exact representation of the control force due to time delays.

The joint damping calculates a torque, $\tau_{D,s}$, equal to:

$$\tau_{D,s} = -D(\eta)\dot{q}_s \tag{3}$$

Such that the total control torque in the joints of the slave, $\tau_s$, is equal to:

$$\tau_s = \tau_{D,s} + J^T F_{K,s} \tag{4}$$

Where J is a Jacobian that describes the kinematics of the slave device.

### B. Estimation of human impedance levels

Humans are able to change the impedance of their limbs in three ways: by changing configuration of the limbs, by applying a force or by co-contracting muscle pairs ([1], [8], [14]). During co-contraction of muscle pairs, the impedance level of the limbs can be changed without changing the limbs configuration or force application. An estimation of the muscle activation levels can be obtained with EMG, which can be related to co-contraction levels.

Exactly determining the quantity of impedance properties of the human arm requires in depth modeling of the human arm. This is a complex task and out of scope for this paper. Given the different structure, scale and mass of a robotic arm some form of mapping human impedance to robot impedance is often required. In this work, a simplified estimation is used; the controller impedance is modulated linearly based on the co-contraction level of the operator.

The co-contraction level is estimated by first collecting a unitless activation level ($\alpha$) of an antagonistic muscle pair that is based on EMG signals. Next, minimum and maximum activation levels of muscles during co-contraction

are calibrated. The minimum level ($\alpha_{min}$) is recorded when the users arm and hand are in a relaxed state, the maximum level ($\alpha_{max}$) is recorded when the user is applying co-contraction at a desired maximum level. These levels are used in normalizing the activation level values with a normalization rule similar to the one utilized by [4]:

$$\hat{\alpha} = \max\left(0, \frac{\alpha - \alpha_{min}}{\alpha_{max} - \alpha_{min}}\right) \tag{5}$$

The maximum of zero and the normalized value is taken to ensure the normalized value never reaches below zero, though this should be prevented as much as possible by selecting an appropriate value for $\alpha_{min}$ . If the normalized activation levels for the flexor and extensor muscles are known through the proposed equation, a normalized co-contraction level ($\eta$) can be determined:

$$\eta = \min\left(1, \hat{\alpha}_{flexor}, \hat{\alpha}_{extensor}\right) \tag{6}$$

Here, $\hat{\alpha}_{flexor}$ is the normalized flexor activation level and $\hat{\alpha}_{extensor}$ is the normalized extensor activation level. Clipping at 1 is included in the equation to prevent the co-contraction level to exceed 100%, which is possible if the activation levels exceed their declared maximum values. By taking the minimum of the normalized flexor and extensor activation levels, their overlapping part is selected - which represents the co-contraction level.

Finally, the co-contraction levels ($\eta$) are low-pass filtered with a cut-off frequency of 5Hz to reduce the effect of high frequency behavior. Additionally, the use of the EMG for impedance modulation is intended as a compensation mechanism for reduced performance due to time delays. Since this signal is subjected to the same time delays it can only be effectively transmitted at relative low frequencies.

### C. Variation law for the controller impedance

The impedance modulation laws that will be used in the research are similar to the ones utilized by [14] and [4] which can be stated independently of the amount of controlled degrees of freedom:

$$\begin{aligned} K(\widetilde{\eta}) &= K_{min} + \widetilde{\eta} \cdot (K_{min} - K_{max}) \\ D_v(\widetilde{\eta}) &= D_{min} + \widetilde{\eta} \cdot (D_{min} - D_{max}) \end{aligned} \tag{7}$$

Here, $\widetilde{\eta}$ indicates a delayed estimate of the co-contraction level of the operators arm. This estimate is delayed because the EMG data is recorded at the master side while the variable impedance controller is located at the slave side. The minimum and maximum stiffness ($K_{min}$ and $K_{max}$, respectively) and damping ($D_{min}$ and $D_{max}$, respectively) values are hardware dependent. Since an accurate model of the hardware is not available for this research, these values were tuned empirically. Both the lower and higher bounds of the impedance levels were defined by the level of transparency of the system. Impedance levels below the defined minimum created a coupling that was experienced as too weak to properly execute tasks, while increasing the impedance levels beyond the set maximum level created stability problems. These problems and possible measures would again decrease the transparency level to an undesirably low level. The determined values for the minimum and maximum stiffness and damping properties are listed in Table I.

Fig. 2: A photo of the experimental setup with: The omega.7 haptic device, Myo armband and a computer screen showing the simulation

TABLE I: Parameter values

| Parameter | Value |
|---|---|
| $K_{min}$ | 100 [$\mathrm{N\,m^{-1}}$] |
| $K_{max}$ | 600 [$\mathrm{N\,m^{-1}}$] |
| $D_{min}$ | 0.2 [$\mathrm{N\,m\,s\,rad^{-1}}$] |
| $D_{max}$ | 0.5 [$\mathrm{N\,m\,s\,rad^{-1}}$] |

### D. Passivity

To guarantee the stability of the control system under time delays and varying control stiffness, a version of the passivity layer approach as described by [6] is applied.

## IV. Experiment design

### A. Experimental setup

The designed controller was implemented on an experimental setup which is shown in Fig. 2 and Fig. 3.

On the master side, an omega.7 ([5]) haptic manipulandum was used to capture motions and feedback forces and a Myo gesture control armband ([12]) was used to capture unitless activation levels ($\alpha$) from the forearm. These activation levels are positive integers, determined by the Myo armband based on recorded EMG signals. Unfortunately, the exact process of this conversion is not publicly available. The telemanipulated environment was simulated with Gazebo (Open Source Robotics Foundation, Mountain View, CA, USA) and visualized on a computer screen. The simulated slave robot was modeled after a LWR4+ robot ([10]). The model was based on the robot model by Research Center E.

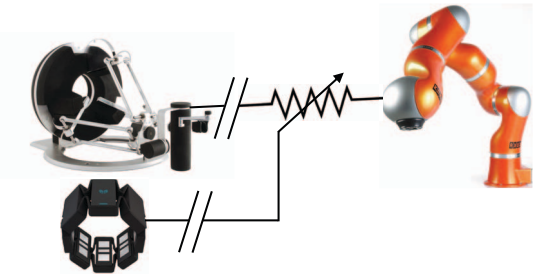

Fig. 3: An overview of the three hardware components, namely; a KUKA LWR4+ as slave device, an omega.7 haptic device as master device and a Myo gesture control armband to acquire muscles activation levels with a schematic representation of the variable impedance controller.

Piaggio at the University of Pisa, Italy[1]. The friction in the model was reduced in order to increase task performance.

### B. Test subjects

The experiments were conducted with a group of ten subjects, of which six were female and four male. The mean of the age of the subjects was 46 (std. 13) years. Eight of the subjects were right handed and two were left handed.

### C. Protocol

The following protocol was followed for each test subject:

1) The subject received a short introduction about the tasks they were going to perform.
2) The subject performed a short calibration task. During the calibration task the maximal and minimal co-contraction levels were determined.
3) The subject performed an experiment that required position accuracy.
4) The subject performed a task that required impact minimization.

Both tasks were performed under six different conditions. The six conditions were all combinations of two different delay settings (no added time delay and 10ms added time delay) and three different impedance settings (low, high and variable). The delays were only added in the communication channel of the controller, not in the visual feedback to the user since an added visual delay of 10ms would not have been perceived by the test subjects ([2]). The order of these variations was randomized within the two experiments, the subjects were not informed on these variations nor on the condition of the current experiment. Subjects were unaware that they could use co-contraction to influence the impedance of the end effector.

Subjects signed an informed consent form before participating in the study. The experimental protocol was approved by the internal committee for research with human subjects at TNO (TC nWMO).

[1]This model is available on the Centro E. Piaggio GitHub: https://github.com/CentroEPiaggio/kuka-lwr

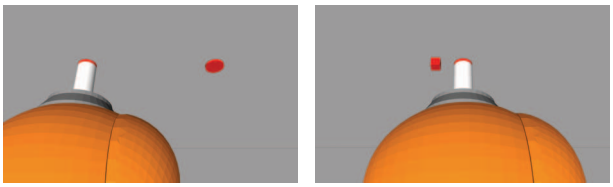

(a) Screen shot of the the positioning accuracy task. The targets are the red cylinders on the screen. One target coincides with the end effector of the simulated robot arm.

(b) Screen shot of the the impact minimization task. The target is the red cylinders on the screen. The block that caused the impact with the end effector is shown left of the end effector. The block was invisible to the test subjects during the experiments.

Fig. 4: Screen shots of the tasks

A detailed description of the calibration procedure and the two experiments is provided in the following subsections.

### D. Calibration procedure

A calibration procedure was used to estimate minimal and maximal co-contraction levels. Every subject was asked to hold on to the omega.7 while the weight of the arm was supported on the table and the Myo armband was worn around the forearm just below the elbow. A multisine reference signal was sent to the omega.7 which tracked this signal with a PD-controller. The multisine signal contained frequencies between 1 and 10 Hz and the subject could not anticipate the progression of the signal. All motions were along the horizontal axis (y-axis) with a maximum amplitude of 25 mm. The subjects received two calibration tasks.

First, the subjects were asked to go along with the motion of the omega.7. During this task subjects were expected to use low co-contraction. The measured activation levels of the relevant muscles were used to quantify the minimum activation levels $\alpha_{min,flexor}$, and $\alpha_{min,extensor}$.

Second, the subjects were asked to keep their hand in the center position, restraining the movement of the omega. During this task subjects were expected to use high co-contraction. The measured activation levels of the relevant muscles were used to quantify the maximum activation levels $\alpha_{max,flexor}$, and $\alpha_{max,extensor}$.

### E. Positioning accuracy task

The first task was aimed at positioning accuracy. In the simulated environment, two clearly visible targets were placed on the y-axis of the end effector. A static camera angle was used that allows the test subject to clearly see the position of the end effector and the targets. A screenshot of the operator's view can be seen in Fig. 4a.

The targets were purely visual and had no physical properties attached to them. The subjects were instructed to move the simulated robot between the targets on an automated spoken rhythm of 'stop' and 'go' commands.

These commands were alternated while spaced in time by 1.5 seconds, creating a constraint on the completion time of every action. Starting at one of the targets, the test subjects were instructed to initiate motion towards the other setpoint at a 'go' command. At the next 'stop' command, the test subjects should have arrived and held the end effector at the next target as accurately as possible until the next 'go' command. Then, the subjects were expected to initiate the motion back to the first target, to arrive here on the next 'stop' command and hold again until the next 'go' command. A total cycle of hitting both targets (go - stop - go - stop) had a total duration of 6 seconds, for each condition ten cycles were recorded.

### F. Impact minimization task

The second task was aimed at compliant movements. Only one target was visible on the screen, the experiment was initialized by the subject positioning the robot approximately at the target. A screenshot of this experiment can be seen in Fig. 4b.

After a keyboard command by the experiment leader, a simulated invisible block of 5 kg traveled towards the simulated end effector. The block traveled along the y-axis (left-right axis) at a velocity of 0.2 m/s, the direction of impact (left or right) and start time after the keyboard command (between 0-3 seconds) were randomly determined. The test subjects were instructed to try to reduce the interaction forces as much as possible without actively moving out of the way of the occuring impact. This means that they were allowed to be pushed to the side by the impacting block. For each condition five impacts were recorded.

### G. Measurements

During the experiments, measurements were conducted on the performance of the task and the co-contraction level of the test subject.

*1) Positioning accuracy task performance:* For the positioning accuracy task, the last five cycles (of the ten recorded cycles per condition) were used to calculate the task performance. The interval between the 'stop' and 'go' commands, in that order, was split into four equal sub-intervals. The mean distance in the second and third sub-intervals (between 25% and 75%) for each cycle was used as the performance indicator. The first and last sub-interval were left out to remove the transient effects.

*2) Impact minimization task performance:* For the impact minimization tasks, the controller forces were used as performance indicator. The controller forces quantified by computing the mean absolute values of the peak controller forces that were applied at each of the five impacts, for all six conditions.

*3) Co-contraction level:* For all experiments, the co-contraction levels were measured with the Myo armband and calculated with the procedure explained in section III. The Myo armband comprises eight sensors that are evenly distributed around the arm. In the experiment, only two sensors were used: sensor 1 that coincided with the Anconeus muscle and sensor 4 that coincided with the Brachioradialis muscle. The pair of sensors estimated the co-contraction level of the elbow flexion-extension direction.

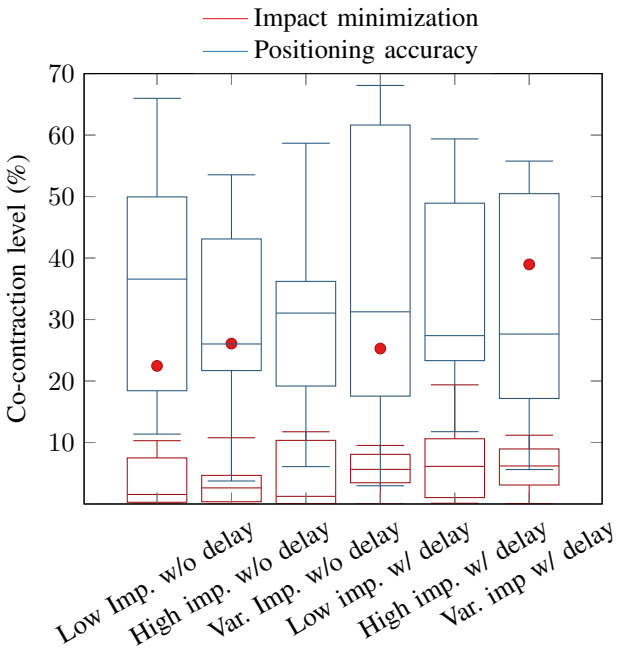


Fig. 5: Co-contraction levels for force and position tasks. Each column shows the results for a position and a force task with the same delay and impedance levels. The top of the box, center mark, and bottom of the box denote respectively the 25th, 50th, and 75th percentile. The whiskers extend to the most extreme points not considered outliers. Outliers are denoted with crosses.

*4) Statistical analysis:* For each measure the mean was calculated. A GML Repeated Measures analysis and a post-hoc analysis using Bonferroni correction was used to analyse the differences of the means of the performance measures (mean distance and peak controller forces). Results with $p < 0.05$ were considered significantly different.

## V. RESULTS

In this section, the measurement results are presented, namely: the co-contraction levels and task performance during both the positioning accuracy and impact minimization tasks.

### A. Co-contraction levels

The co-contraction levels during the experiments are shown in Fig. 5. The results in Fig. 5 show that the co-contraction was lower during the execution of the impact minimization tasks compared to the positioning accuracy For all conditions, the difference is significant ($p < 0.005$, paired t-test).

### B. Task performance

The performance during the positioning accuracy and impact minimization tasks is shown in Fig. 6. Results of pairwise comparison are shown in Table II.

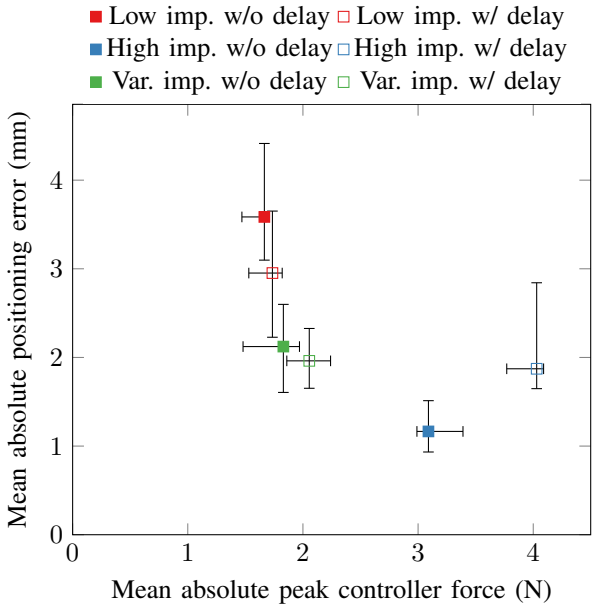


Fig. 6: Task performance with different impedance levels and delays. Points denote the median value. The whiskers extend to the 25th and 75th percentile.

TABLE II: Pairwise comparisons

Mean differences that are significant at the 0.05 level are denoted with a *. Bonferroni correction is used to adust for multiple comparisons.

**IMPEDANCE LEVEL**

| | | **Positioning accuracy** | | **Impact minimization** | |
|---|---|---|---|---|---|
| | | Low | High | Low | High |
| p-value | Variable | 0.048∗ | 1.000 | 0.009∗ | 0.000∗ |
| | High | 0.031∗ | X | 0.000∗ | X |

**ADDED DELAY**

| | | **Positioning accuracy** | **Impact minimization** |
|---|---|---|---|
| | | Without | Without |
| p-value | With | 0.132 | 0.000* |

The pairwise comparison of impedance levels showed significant differences for all but one tasks ($p < 0.05$, except high vs. variable impedace in the positioning accuracy task). The pairwise comparison of delay settings showed a significant difference for the impact minimization task, but not for the positioning accuracy task.

For the condtions without time delay, the smallest error in the positioning task was achieved with the high impedance (median was 1.17 mm), the variable impedance scored second (2.12 mm), the low impedance had the largest error (3.59 mm). For the force task this was the opposite. The smallest peak controller force was achieved with the low impedance task (1.67 N), the variable impedance scored second (1.83 N), the high impedance had the largest peak forces (3.09 N). For the conditions with time delay approximately the same pattern was observed. Errors for the position task were 1.87 mm, 1.96 mm, and 2.96 mm for respectively the high, low, and variable impedance. Errors in force task were 4.03 N, 2.05 N and 1.73 N for respectively the high, low and variable impedance.

## VI. DISCUSSION

The first hypothesis was that telemanipulation tasks that require high position accuracy are performed better with high impedance, and telemanipulation tasks that require impact minimization are performed with low impedance. The results from the experiments confirmed this hypothesis.

The second hypothesis was that co-contraction in a telemanipulation task that require high positioning accuracy is higher than for tasks that require impact minimization. It was shown that for all conditions the co-contraction in the positioning accuracy task was higher than for the impact minimization task.

The third hypothesis was that scaling impedance with co-contractions allows users to effectively change between high and low impedance. All conditions were pareto optimal. For the position task the variable impedance task scored relatively close to the high impedance condition and for the force task the variable impedance scored relatively close to the low impedance condition. [1], [14] found the same relation; position tasks requiring high impedance and force tasks requiring low impedance, with variable impedance controllers that used respectively grasping force with haptic feedback and EMG without haptic feedback, respectively. This is a strong indication that co-contraction was effectively used to adapt the impedance level to the task requirements. For the conditions with added time delay we could not draw the same conclusion due to the lack of statistical significance.

It was expected that time delay had a large influence on task performance. However, in the experimental results only minor differences were noticed. This could be partly due to the fact that time delays were relatively small in the experiments. Additionally, for consistency, the same values for $K_{min}$, $K_{max}$, $D_{min}$, $D_{max}$ were used for the conditions with and without added delay. However, this choice might not have resulted in optimal performance for all conditions.

Notwithstanding the positive results, some remarks have to be made and some issues have to be solved before the method could be widely applied.

In the impact minimization task, the subject did not use the force feedback for their task. To see the effect of variable impedance in combination with force feedback other tasks can be evaluated. An example of such a task is given by [14]. During this task, the subjects have to carefully touch a wall and apply a target force afterward.

Both experiments comprised a 1-DoF task in a limited range of motion. It was therefore sufficient to have a relative course estimate of the co-contraction for two antagonist muscles. If the experiment is extended to multiple dimensions the complex structure of the human arm has to be considered. A model of the human arm might be needed that couples muscle geometry to specific degrees of freedom ([1]).

## REFERENCES

[1] A. Ajoudani, N. Tsagarakis, and A. Bicchi, "Tele-impedance: Teleoperation with impedance regulation using a body-machine interface,"

*International Journal of Robotics Research*, vol. 31(13), pp. 1642–1655, 2012.

[2] K. Asli, V. Lotte, E. S. A., D. Pieter, P. Ljiljana, V. N. Yves, V. D. W. Nele, J. An, V. L. Jan, and P. Wilfried, "Effect of video lag on laparoscopic surgery: correlation between performance and usability at low latencies," *The International Journal of Medical Robotics and Computer Assisted Surgery*, vol. 13(2), p. 1758.

[3] A. Brygo, I. Sarakoglou, N. Tsagarakis, and D. Caldwell, "Tele-manipulation with a humanoid robot under autonomous joint impedance regulation and vibrotactile balancing feedback," in *IEEE-RAS International Conference on Humanoid Robots*, vol. 2015-February, 2015, pp. 862–867.

[4] J. Chen, M. Glover, C. Li, and C. Yang, "Development of a user experience enhanced teleoperation approach," in *ICARM 2016 - 2016 International Conference on Advanced Robotics and Mechatronics*, 2016, pp. 171–177.

[5] Force Dimension website, "omega.7 product overview," retrieved June 14th 2017. [Online]. Available: http://www.forcedimension.com/products/omega-7/overview

[6] M. Franken, S. Stramigioli, S. Misra, C. Secchi, and A. Macchelli, "Bilateral telemanipulation with time delays: A two-layer approach combining passivity and transparency," *IEEE Transactions on Robotics*, vol. 27(4), pp. 741–756, 2011.

[7] K. Hashtrudi-Zaad and S. Salcudean, "Analysis of control architectures for teleoperation systems with impedance/admittance master and slave manipulators," *International Journal of Robotics Research*, vol. 20(6), pp. 419–445, 2001.

[8] M. Hill and G. Niemeyer, "Real-time estimation of human impedance for haptic interfaces," in *Proceedings - 3rd Joint EuroHaptics Conference and Symposium on Haptic Interfaces for Virtual Environment and Teleoperator Systems, World Haptics 2009*, 2009, pp. 440–445.

[9] J. Kim, P. Chang, and H.-S. Park, "Transparent teleoperation using two-channel control architectures," in *2005 IEEE/RSJ International Conference on Intelligent Robots and Systems, IROS*, 2005, pp. 2824–2831, cited By 18.

[10] KUKA Roboter GmbH, *Lightweight Robot 4+ Specification*, Dec. 2012, Version: Spez LBR+ V6 en (PDF), Issued 17.12.2012.

[11] D. Lawrence, "Stability and transparency in bilateral teleoperation," *IEEE Transactions on Robotics and Automation*, vol. 9(5), pp. 624–637, 1993.

[12] Myo website, "Myo Tech Specs page," retrieved June 21th 2017. [Online]. Available: https://www.myo.com/techspecs

[13] E.-C. Shin, J.-H. Ryu, and G.-H. Yang, "Estimation of human arm impedance in accordance with the master device types and gripping posture," in *IEEE/ASME International Conference on Advanced Intelligent Mechatronics, AIM*, vol. 2015-August, 2015, pp. 1744–1748.

[14] D. Walker, R. Wilson, and G. Niemeyer, "User-controlled variable impedance teleoperation," in *Proceedings - IEEE International Conference on Robotics and Automation*, 2010, pp. 5352–5357.